Journal of Electroanalytical Chemistry 965 (2024) 118373

Contents lists available at ScienceDirect

Journal of Electroanalytical Chemistry

journal homepage: www.elsevier.com/locate/jelechem

Identification of electrochemically formed metal oxides by coupling high-temperature cyclic voltammetry with Raman spectroscopy

Michael Georg Stadt [a,b,*], Silvia Larisegger [b], Michael Nelhiebel [c], Günter Fafilek [a]

[a] TU Wien, Institute of Chemical Technologies and Analytics, Getreidemarkt 9/164-EC, 1060 Vienna, Austria
[b] KAI Kompetenzzentrum Automobil- und Industrieelektronik GmbH, Argentinierstraße 8, 1040 Wien, Austria
[c] KAI Kompetenzzentrum Automobil- und Industrieelektronik GmbH, Technologiepark Villach Europastraße 8, 9524 Villach, Austria

ARTICLE INFO

Keywords:
High-temperature cyclic voltammetry
Raman spectroscopy
Electrochemically controlled oxidation

ABSTRACT

High-temperature cyclic voltammetry (HT-CV) is a versatile technique for accurately characterizing metal oxidation processes. This method uses YSZ (Yttria-stabilized zirconia), a solid-state oxygen ion conductor, as an electrolyte. By applying defined potentials, different oxide species are produced. Hence, thermodynamic processes such as the stability of oxides and kinetic properties, like growth rates, can be investigated. However, in electrochemical reactions the current cannot be assigned to specific reactions unequivocally. To address this issue, *in situ* analytical methods are necessary. This is crucial when investigating diffusion processes and reaction products, as they require additional analytical information.

This work presents a novel method that combines high-temperature electrochemistry with Raman spectroscopy to investigate metal oxidation processes and diffusion phenomena directly at the solid-electrolyte/metal interface. The HT-CV method is used to achieve controlled oxidation states of metals. To this end, a commercial Raman heating stage was adapted to enable electrochemical measurements in the cell. The use of a transparent YSZ single crystal allows Raman measurements, as the laser penetrates through the material to the metal (oxide)/electrolyte interface. With Raman spectroscopy, oxides produced under controlled conditions can be analyzed. Furthermore, optical microscope images of the oxides can be taken during their formation. Our combined method also enables the investigation of metallic interdiffusion. The electrochemical control of the potential allows for the selective oxidation of diffusing species whilst the layer through which the diffusion takes place remains in the reduced state. The results obtained with Raman spectroscopy confirm the existence of the species predicted from electrochemical experiments.

1. Introduction

The oxidation behavior and mechanisms of different metals is of significant interest in almost every industry sector. In numerous applications, metals are exposed to elevated temperatures both during production and during actual use. Clarification of the ageing processes is crucial for designing metals with preferable, defined properties. In addition, diffusion phenomena are strongly influenced by temperature. A simple and robust method is desirable to determine the diffusion of metals through metal barrier layers.

Commonly, metal oxidation is investigated by oxidizing the sample under defined conditions (i.e., oxygen concentration and temperature) and subsequent chemical analysis [1,2]. However, this procedure is very extensive and time-consuming. Furthermore, it is challenging to conclude the kinetics of the oxidation process, as only the final state can be accessed for analysis. This is particularly important for metals that can form more than one oxide, e.g. copper: Cu_2O/CuO.

High-temperature cyclic voltammetry (HT-CV) is a method for the controlled oxidation of metals [3–5]. In HT-CV, the potential controls the oxygen partial pressure at the solid electrolyte/metal interface. In this work, a single-crystal of yttria-stabilized zirconia (YSZ) is utilized as an oxygen ion conducting electrolyte. HT-CV has been used to investigate the oxidation behavior of materials ranging from metals and alloys [6] to materials, e.g., for SOFC applications. Thereby, the kinetic and thermodynamic properties of the mechanism can be studied during the oxidation. However, electrochemical techniques require some complementary analytical information. In almost every electrochemical experiment, several processes contribute to the measured current

* Corresponding author.
E-mail address: michael.stadt@tuwien.ac.at (M.G. Stadt).

https://doi.org/10.1016/j.jelechem.2024.118373
Received 8 March 2024; Received in revised form 10 May 2024; Accepted 20 May 2024
Available online 21 May 2024

simultaneously. Therefore, an analytical measurement should be performed concurrently with the electrochemical oxidation.

One such complimentary technique is Raman spectroscopy. Raman spectroscopy allows the distinction between the different oxidation states of metals. In liquid systems, *in situ* Raman spectroscopy has been performed on copper and its oxides [7]. However, compared to HT-CV, where pure oxides are formed, an aqueous electrolyte leads to a higher number of possible compounds that can form, such as $Cu(OH)_2$ and $NaCuO_2$ [7]. Single crystals of YSZ are optically transparent, allowing visible light to pass through. Therefore, confocal Raman spectroscopy is the method of choice for analyzing oxidic species through the solid electrolyte. The confocal arrangement enables focusing on thin layers. For our HT-CV measurements, Raman spectroscopy was chosen as complimentary techniques, since the measurements can be performed through the optically transparent ionic conductor.

In this work, different metals and metal layer structures are oxidized under electrochemical control. The different oxidation states, produced by HT-CV, are preserved by cooling down under electrochemical control. Subsequently Raman spectroscopy and optical microscopy are performed. The oxidation and reduction current peaks observed during HT-CV can thus be reliably assigned to specific oxides. In general, metals are not Raman-active, whereas oxides show Raman scattering.

In the semiconductor industry, titanium is used as a metal barrier layer between the silicon substrate and the conductive (structured) gold top-layer to prevent interdiffusion [8–13]. However, above temperatures of 250 °C diffusion of titanium through gold is observed [9]. Our novel method can be utilized for the electroanalytical analysis of the stability of such barrier layers. Initially, the intact gold top layer does not show Raman scattering. A potential is applied at which the less noble metals (e.g. Ti), which are supposed to diffuse toward the surface, are oxidized at the surface. The more noble top layer (e.g. Au) remains in the metallic state. The oxidized, diffused species at the surface can then be detected by Raman spectroscopy.

2. Materials and methods

Single crystalline yttria-stabilized zirconia (YSZ) is used as a solid electrolyte in high-temperature cyclic voltammetry. It is conductive for oxygen ions at elevated temperatures with a value of $3{\cdot}10^{-6}$ S/cm at 300 °C and about $2{\cdot}10^{-2}$ S/cm at 750 °C [14]. HT-CV is carried out in a three-electrode arrangement, with the Raman laser irradiating the sample through the optically transparent YSZ (Fig. 1). The working electrode (WE) is the metal of interest. Two types of samples were used. Depending on the sample type, either spherical/cuboid metal electrodes or sputtered metal layers were used as WE (Fig. 2). Platinum metal, molten to a spherical shape, is used as the reference electrode (RE). The counter electrode (CE) consists of a porous, burnt-in layer of platinum. The top of the solid electrolyte is entirely covered by the porous platinum, except for a small hole for the Raman laser. The whole arrangement is placed in a gas-tight chamber with a constant argon flow. Thereby, a constant, known oxygen partial pressure, $p_{O_2}^{res}$, equal to the amount of residual oxygen in the argon is reached. By applying a defined potential, the oxygen partial pressure at the metal surface can then be adjusted, according to the Nernst equation (Equation (1) [15].

$$\Delta E = \frac{R \cdot T}{z \cdot F} ln \left[\frac{p_{O_2}}{p_{O_2}^{res}} \right] \quad (1)$$

In this equation, R is the ideal gas constant, T is the temperature and F the Faraday constant. The number of transferred electrons is represented by z and p_{O_2} is the oxygen partial pressure at the solid electrolyte/metal interface. Performing cyclic voltammetry (CV) leads to the reversible oxidation of the metal and reduction of the oxides. The current is proportional to the amount of metal converted into oxide and vice versa. All mentioned potentials are calculated against the reversible electrode in pure oxygen (ROE). All potentials in the diagrams and in the text refer to this reference potential. The electrochemical measurements were carried out using a Methrom Autolab PGSTAT128N potentiostat.

A commercially available Raman heating stage from Linkem® was used for the coupled electrochemistry-Raman measurements. Fig. 2 shows a schematic representation of the setup inside the heating cell for the two different sample geometries. The heating block inside the stage is made of silver, which enables efficient heating. Three gold-coated tungsten needles are utilized to establish electrical contact, one for each electrode. The needles are also used to press the solid electrolyte onto the sample. The needles can be placed freely in the chamber using magnets and are connected to the outside via BNC sockets. A milled alumina block contained recesses to hold the working electrode and reference electrode. Molten metal spheres (Cu, Ni), cubes cut from sheet metal (Ti) as well as sputtered metal layers (Au/Ti) on conductive silicon were used as samples. Metal spheres with diameters of approximately 0.5 mm were produced by melting wires with a purity of 99.99 %. The surface oxide was then etched away using 4 mol/L sulfuric acid. The spherical shape and soft nature of the samples allowed for the formation of a small contact area between the metal and the solid electrolyte by slight deformation upon pressing the YSZ onto the sphere, as shown in Fig. 2. The cubic, metallic titanium samples were cut out of a metal plate with 5 mm thickness. The layers for the gold-titanium samples were

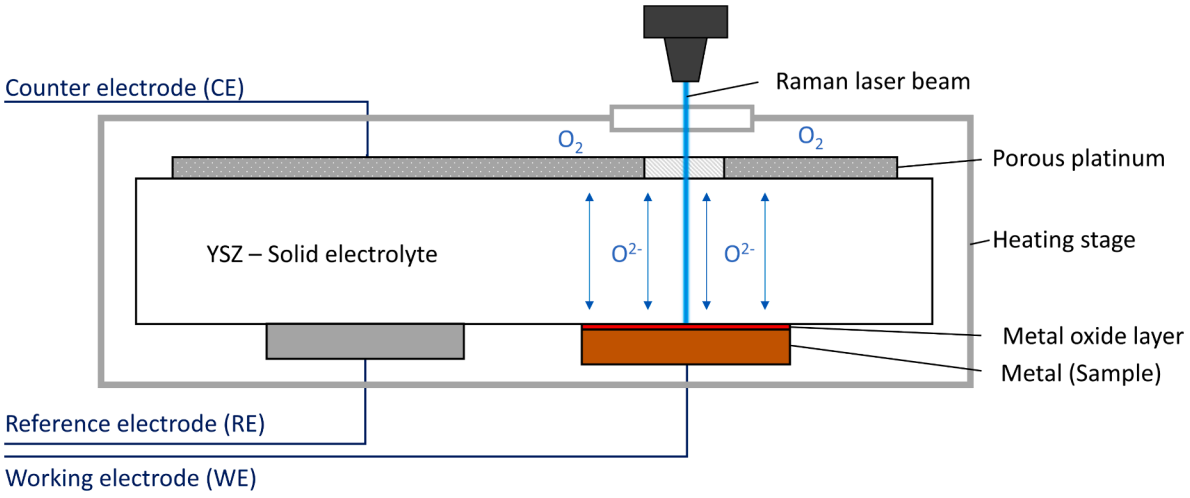

Fig. 1. Schematic layout of the three-electrode arrangement for HT-CV with *in situ* Raman spectroscopy. The Raman laser irradiates the oxide through the solid electrolyte. A modified heating stage is used to control the temperature.

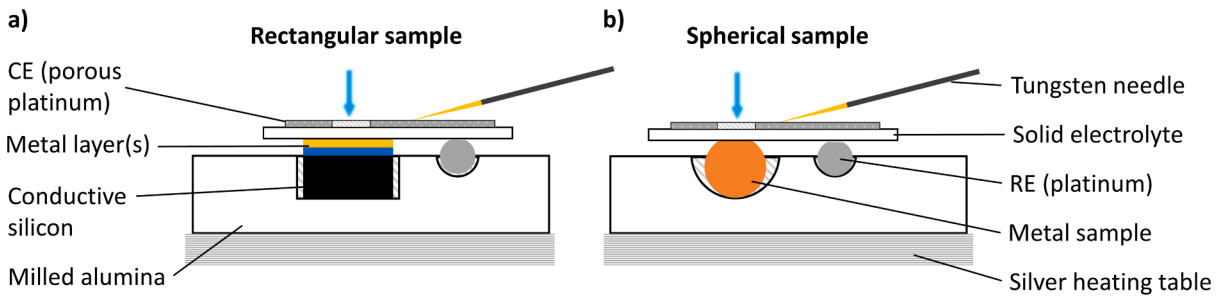

Fig. 2. Schematic setup inside the heating stage with the two possible arrangements: a) Rectangular samples: metallic or sputtered metal layer on a conductive substrate. b) Spherical metallic samples.

produced by cold sputtering the metals onto a conductive silicon substrate.

For the Raman measurements presented in this work, a WITEC alpha300RSA + confocal microscope was used. A blue laser with a wavelength of 488 nm was used at 5–50 mW energy within a 50x extra-long working distance (ELWD) objective. The long working distance is required to be able to focus inside the cell. However, our setup for the *in situ* Raman spectroscopy in a solid-state configuration is inherently associated with a few disadvantages:

- Stokes scattering becomes less intensive at higher temperatures: The used Raman device is equipped with an edge filter, which only gives access to Stokes scattering. Anti-Stokes scattering increases in intensity at high temperatures, but is inaccessible with our device.
- Focusing the laser beam through the heating-stage cover glass and the YSZ-solid electrolyte: The laser beam has to be focused through the quartz cover glass of the heating stage and the solid electrolyte. Therefore, the light is scattered four times on its way to the sample and back to the detector (i.e. cover glass–YSZ–metal oxide–YSZ–-cover glass). Electropolished single crystalline YSZ with a roughness of Ra < 0.5 nm was used to minimize these negative scattering aspects. However, as seen in Fig. 5, this still leads to blurry microscopic images.
- The solid electrolyte YSZ is Raman active: Amongst all oxygen ionic conducting electrolytes, YSZ is the only one that can be produced as an optically transparent single crystal with a sufficient size ($>3 \times 3$ mm^2). Even though confocal-Raman is applied, the focus on the oxide/electrolyte interface leads to the excitement of both the oxide and the solid electrolyte [16].

The high temperature (>300 °C) poses the most significant issue for obtaining Raman spectra of the oxides. To mitigate the temperature-related problems, the oxide is cooled in a controlled way to maintain the defined, electrochemically formed oxides. Therefore, during cool-down, the applied potential is shifted with the decreasing temperature (Fig. 3a) to maintain the thermodynamically defined oxidation state. A step-wise adjustment of the potential was used, approximating the calculated potential curve. The potential was adjusted every 50 s, as displayed in Fig. 3b. As the temperature drops rapidly in the first 50 s at a rate of over 150 °C/minute, the further redox reaction during cooling is only marginal.

3. Results and discussion

3.1. High-Temperature cyclic voltammograms of metal oxides

High-temperature cyclic voltammograms of metals reveal the stability ranges of their oxides. Every cyclic voltammogram (CV) consists of oxidation peaks (referred to as Ox) and reduction peaks (referred to as Red). The number of peaks depends on the number of possible oxides and the scanned potential range. The possible redox couples for the different investigated metals are displayed in the table in Fig. 4d. Each oxide is stable within a specific potential (=oxygen partial pressure) range. These stability ranges can be calculated using thermodynamic data. Fig. 4a–c displays the cyclic voltammograms of copper, nickel, and titanium recorded at 550 °C at a scan rate of 10 mV/s. The arrows at the bottom x-axis indicate the calculated stabilities for the oxides. The redox potentials of the different redox pairs were calculated using thermodynamic data from literature [17]. Following Equation (2), the Gibbs free energy of a reaction can be converted into an electrochemical potential ΔE. The potential vs. ROE, plotted on the x-axis, can be converted into the oxygen partial pressure (top x-axis) by using the Nernst equation

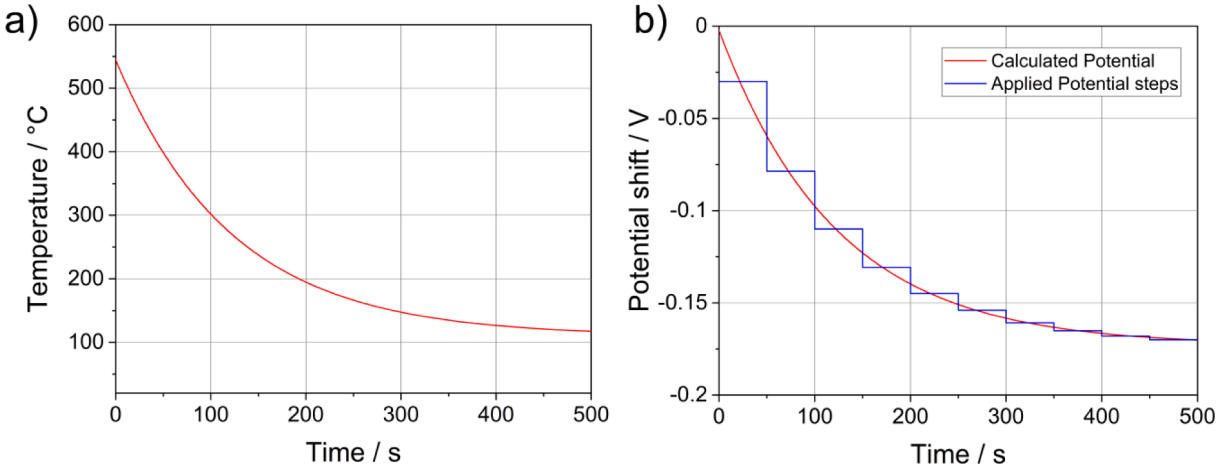

Fig. 3. a) Cooling curve of the Raman heating stage. b) Red: potential shift with respect to the potential at 550 °C to maintain the defined oxidation state. Blue: Step-wise approximation of the potential shift.

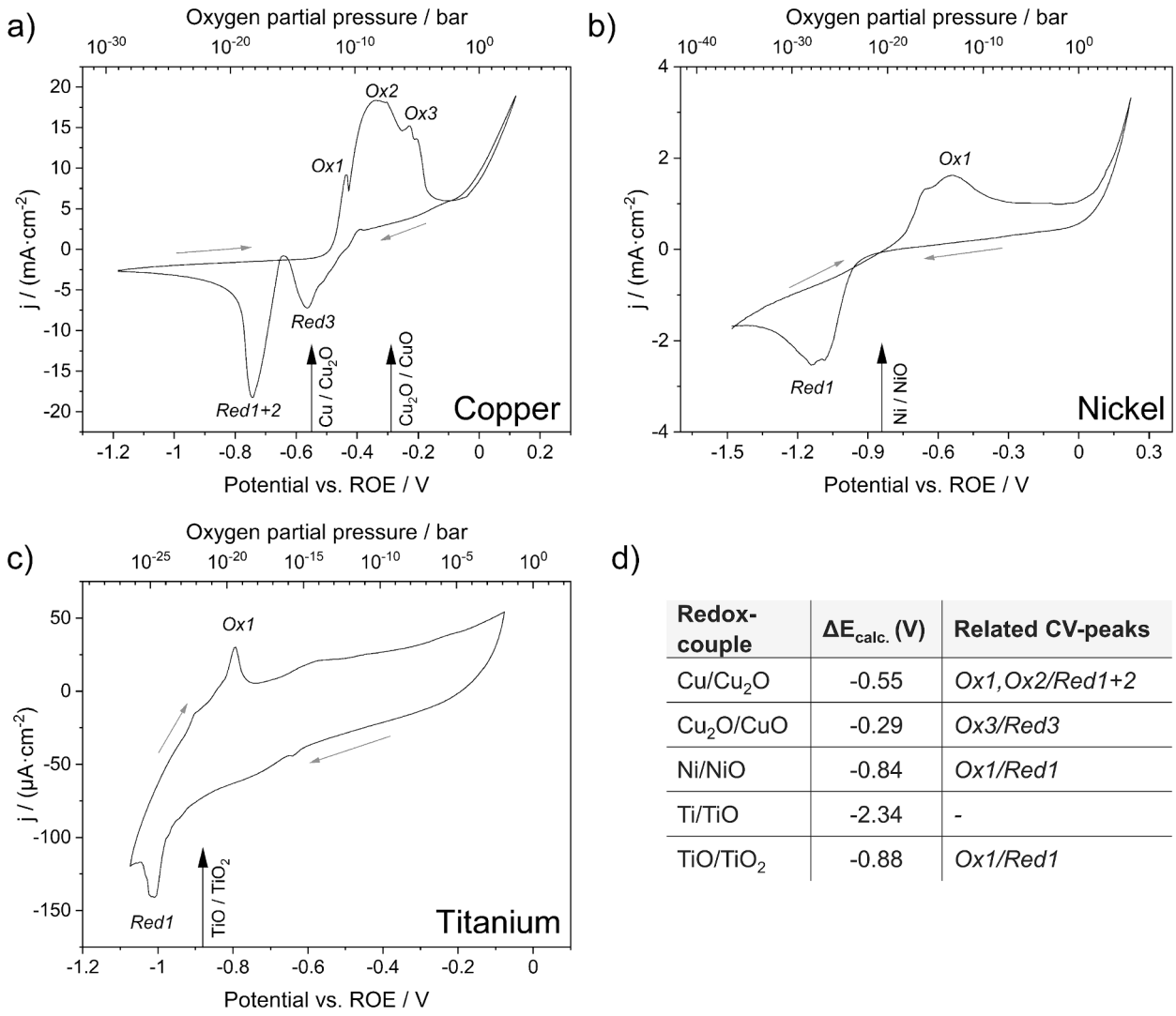

d)

Redox-couple	$\Delta E_{calc.}$ (V)	Related CV-peaks
Cu/Cu_2O	-0.55	*Ox1,Ox2/Red1+2*
Cu_2O/CuO	-0.29	*Ox3/Red3*
Ni/NiO	-0.84	*Ox1/Red1*
Ti/TiO	-2.34	-
TiO/TiO_2	-0.88	*Ox1/Red1*

Fig. 4. Cyclic voltammograms at 550 °C and a scan rate of 10 mV/s. Recorded in the Raman heating cell modified for electrochemical measurements: a) Copper, b) Nickel, c) Titanium. d) Calculated potentials for the redox pairs of the metal oxides at 550 °C.

Equation (1).

$$\Delta E = -\frac{\Delta G}{z \cdot F} \tag{2}$$

In Eq. (2), z is the number of transferred electrons, F the Faraday constant and ΔG the Gibbs free energy. At potentials above around 0 V, the current increases in the CVs as the oxygen evolution reaction starts. This phenomenon occurs in all measurements displayed in Fig. 4a–c, regardless of the metal.

Copper

$$2Cu + O^{2-} \rightleftarrows Cu_2O + 2e^- \quad \Delta E = -0.55V$$
$$Cu_2O + O^{2-} \rightleftarrows 2CuO + 2e^- \quad \Delta E = -0.29V$$

The cyclic voltammogram of copper shows three oxidation and two reduction peaks for the two known oxidation states, Cu(I) oxide and Cu (II) oxide. The occurrence of three oxidation peaks can be explained, since during the initial oxidation of the copper metal to Cu(I) oxide, a thin passivation layer is formed, resulting in the pre-peak Ox1 [18]. After this layer has been formed, Cu is further converted to Cu_2O (Ox2). The third oxidation peak, from Cu(I) to Cu(II), is superimposed by the second oxidation peak. At much slower scan rates, the separation of the peaks is improved, i.e. below 1 mV/s.

Nickel

$$Ni + O^{2-} \rightleftarrows NiO + 2e^- \quad \Delta E = -0.84V$$

Nickel oxide has only one oxidation state (nickel(II) oxide) within the scanned potential range. In the CV one oxidation and one reduction peak are visible. The current in the cyclic voltammogram of nickel is one order of magnitude lower than that of copper. As nickel is much harder, a smaller contact area is obtained upon pressing the solid electrolyte onto the metal. Furthermore, nickel forms a highly resistive oxide layer which leads to a reduction in current [15].

Titanium

$$Ti + O^{2-} \rightleftarrows TiO + 2e^- \quad \Delta E = -2.34V$$
$$TiO + O^{2-} \rightleftarrows TiO_2 + 2e^- \quad \Delta E = -0.88V$$

In terms of HT-CV, metallic titanium is stable only at potentials below −2.32 V, which cannot be reached using YSZ as an electrolyte. The YSZ would be reduced itself before reaching such low potentials. Therefore, the titanium oxidation and reduction peak in Fig. 4c show the transition from TiO to TiO_2 and vice versa.

3.2. *In operando optical microscopy of metal oxides*

Microscopic images of the electrochemically formed oxide species

during HT-CV were recorded *in operando*. The transparent solid electrolyte allows to obtain images during their electrochemically controlled formation. Microscopic images were taken of the different oxidation and reduction states described in the previous chapter (Fig. 4). For these pictures, the focused light passes the glass of the heating-stage cover and the transparent singly-crystalline electrolyte. Therefore, the light is scattered four times (i.e. cover glass–YSZ–metal oxide–YSZ–cover glass), resulting in partially blurry images. However, the different metal oxides clearly show different colors, as expected. The copper and nickel spheres only show the oxidation reaction at the small metal/solid electrolyte contact area. For titanium, the metallic state is only present before the first oxidation step, as it can only be reduced from TiO_2 to TiO with the utilized solid electrolyte. Furthermore, titanium was used as a sputtered layer, as it cannot be molten into a sphere in a conventional oxyhydrogen flame. **Copper:** As copper is a soft metal, a large contact surface is created when the flat electrolyte is pressed onto the metal ball. The different states of copper (i.e., metallic, copper(I), and copper(II)) can be clearly distinguished optically. In the metallic state, a reddish color is visible. Cu_2O and CuO appear in their true colors which are orange/red for Cu_2O and black for CuO. **Nickel:** With the harder nickel, only a small contact area is formed when pressed onto the electrolyte. Still, the oxidized and reduced state could be spotted since nickel has a grayish appearance, and nickel(II) oxide is darker. **Titanium:** Titanium always has a passive layer under ambient conditions. The layer, however, is so thin that it is not optically visible. This "native metallic state" was already present before the controlled oxidation at elevated temperatures. Once the titanium is oxidized, it cannot be reduced from TiO to Ti with HT-CV anymore. The colorless TiO_2 appears in blue interference colors. The edge in the titanium pictures in Fig. 5 represents the edge of the silicon substrate. Due to the construction of the heating cell, the best contact between the metal and the solid electrolyte is achieved at the edge of the substrate.

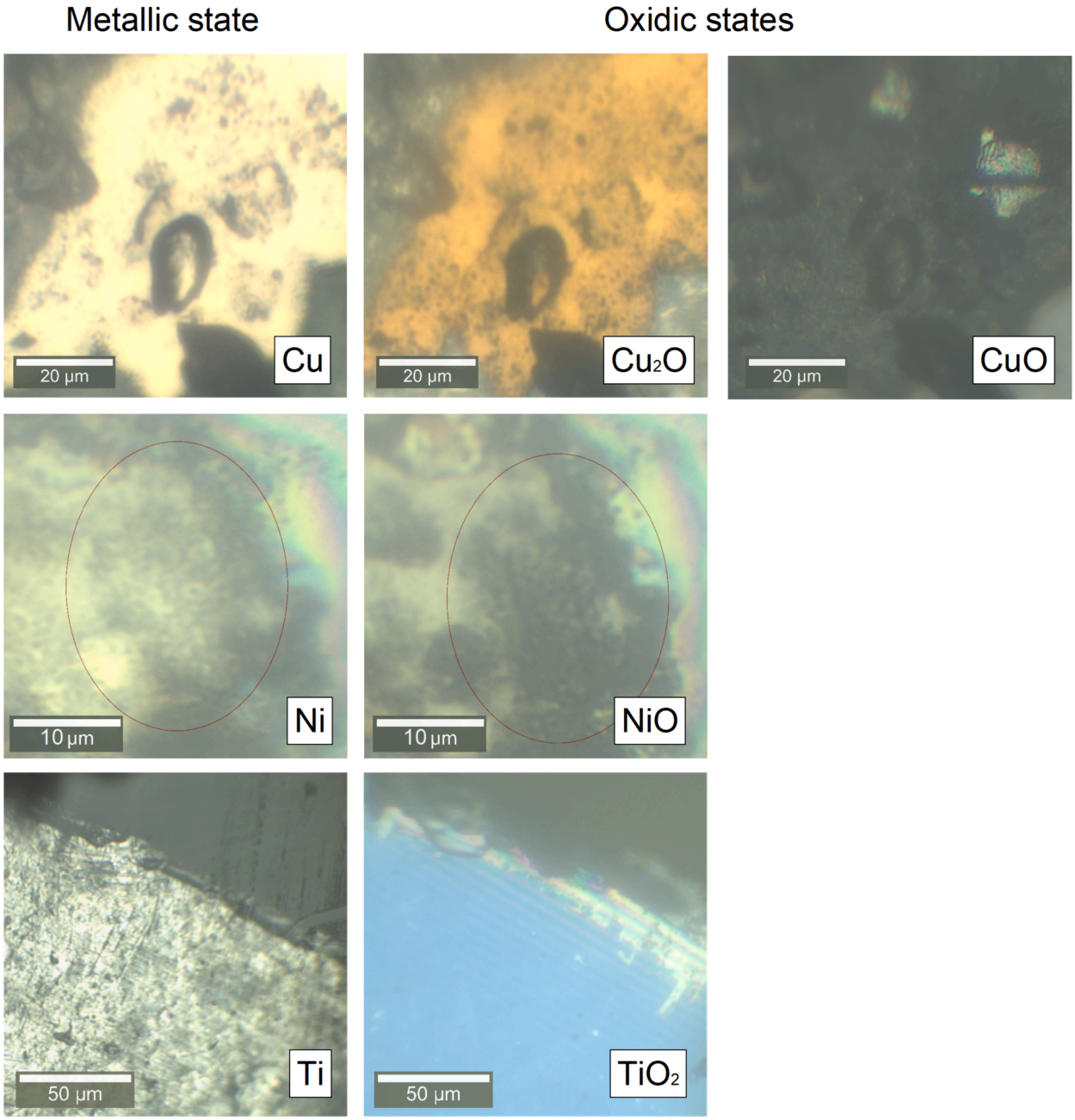

Fig. 5. In operando microscopic images of the different metals and their oxides (obtained at a 50x magnification).

3.3. Raman spectroscopy

Raman spectroscopy was performed to confirm the electrochemically formed oxides by an analytical method without detaching the electrochemical setup. We found that at temperatures exceeding 300 °C, which are required for electrochemical oxidation, it was not possible to obtain satisfactory Raman spectra. Therefore, the defined oxides were cooled to room temperature under electrochemical control, in order to obtain reliable Raman spectra.

3.3.1. *In situ* Raman spectra at elevated temperatures

Initially, Raman spectra of the oxides were acquired *in situ* directly during the HT-CV measurements at high temperatures. As the intensity of the Stokes scattering decreases with increasing temperature, the total Raman signal is substantially lower than at room temperature. However, at temperatures above 300 °C, which are needed to obtain satisfactory electrochemical data, the solid electrolyte completely overlaps the oxidic Raman peaks. Note, that YSZ shows a broad range of Raman scattering in the Region from 100 cm^{-1} to 600 cm^{-1} (see Fig. 6). Most metals also show their main Raman bands in this region. Hence, the introduced method with electrochemically controlled cooldown for preserving the oxidation state, as explained in the materials and methods section (Chapter 2, Fig. 3), was used.

3.3.2. Raman spectra at room temperature after electrochemically controlled cooldown

The Raman measurements of the defined oxides were carried out at room temperature to obtain identifiable spectra. For each of the four oxides, the respective Raman spectrum shows at least one characteristic Raman band (see Fig. 6). Since all spectra were recorded through the solid electrolyte, each oxide spectrum contains vast contributions from the YSZ Raman spectrum. The utilized YSZ from CrysTec GmbH shows Raman scattering in the 100 cm^{-1} to 600 cm^{-1} range with two distinct bands at 150 cm^{-1} and 625 cm^{-1}. The spectrum is denoted as YSZ Ref. in Fig. 6. **Copper:** Copper(I) oxide has its most intense Raman signal at the second-order overtone at 218 cm^{-1} [19]. Copper(II) oxide exhibits its main vibrational mode (A_g) at 282 cm^{-1} [20]. The YSZ spectrum covers all further Raman modes of the two copper oxides. In the Cu_2O spectrum, a small CuO peak at 282 cm^{-1} can be found. During the cyclic oxidation and reduction in HT-CV an incomplete conversion is observed. This suggests minor changes in the surface morphology of the material, which changes the contact area between the oxides and the electrolyte. **Nickel:** The Raman spectrum of nickel oxide exhibits three bands in the range from 900 cm^{-1} to 1500 cm^{-1}, which can be assigned to the two-phonon modes (906 cm^{-1} and 1090 cm^{-1}) and the two-magnon scattering at ~ 1500 cm^{-1} [21]. These shifts can be identified more clearly, as they are not overlapping with the YSZ Raman scattering. **Titanium:** The thermal oxidation of titanium on different substrates at temperatures of 500–700 °C is described in literature [22–24]. X-Ray diffraction analysis (XRD) has shown that at these temperatures Ti_6O and the rutile phase (TiO_2) are formed [22]. Raman spectroscopy provides even more detailed information about structural features. As an example, slight wavelength shifts are obtained and detected by isotopic exchange of ^{16}O by ^{18}O in the anatase structure of titanium dioxide [25]. Further,

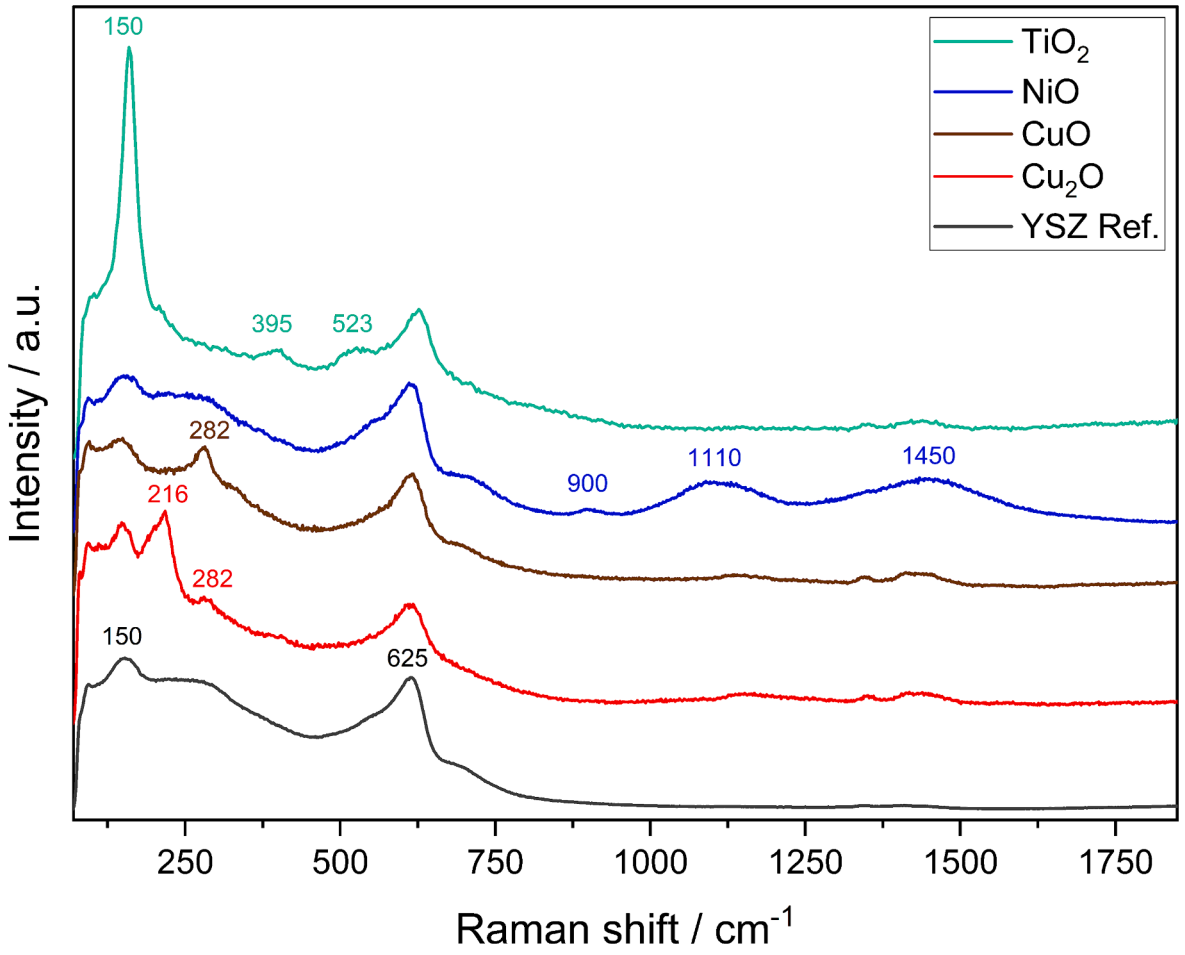

Fig. 6. Raman spectra of YSZ (black, background reference) and the different oxides after the electrochemically controlled cooldown in the heating stage: TiO_2 (turquoise), NiO (blue), CuO (brown) and Cu_2O (red). The spectra are offset for clarity and the intensity scale is zoomed by different factors (TiO_2:1.5; NiO:1; CuO:1.1; Cu_2O:1.2; YSZ:0.09).

structural changes during insertion of lithium into anatase were determined *in situ* by Raman spectroscopy [25]. Despite these abilities of Raman spectroscopy described in the literature, in our solid-state electrochemical cell, the Raman signal of the YSZ electrolyte overlaps with most of the anatase peaks. Therefore, such detailed information cannot be extracted from our Raman spectra. However, the dominant phonon mode $E_g(1)$ which is located at 144 cm^{-1} [26] indicates, that in contrast to the thermal oxidation [22,24], the HT-CV method at 550 °C leads to the formation of the anatase phase. The preferential formation of the anatase phase might be due to the higher oxidation rate or the electrochemical oxidation mechanism in our HT-CV solid-electrolyte experiment. The Raman spectrum of the sample also shows the presence of other active Raman modes typical of the anatase phase, namely the $B_{1g}(1)$ mode at 394 cm^{-1}, $B_{1g}(2)$ mode at 516 cm^{-1} and $E_g(3)$ at 638 cm^{-1} [27]. However, the formation of rutile cannot be completely ruled out due to the high baseline from the solid electrolyte. All modes are consistently shifted to higher wavenumbers (~6 wavenumbers). The shifts of the $B_{1g}(1)$ and $B_{1g}(2)$ modes agree with the shift of the dominant mode. This verifies the presence of titanium as the main mode around 150 cm^{-1} which almost matches the Raman shift of the solid electrolyte.

4. Application: Diffusion of titanium through a gold layer

The stability of barrier layers is crucial in semiconductor manufacturing, where different metals are used as barrier layers to prevent the diffusion of other metals [28–30]. Titanium films are often used as adhesion and/or barrier layer between metallic layers and silicon substrates, and have therefore already been investigated using several methods [9,12,13]. For this purpose, samples with sputtered metal layers on a conductive silicon substrate were produced by depositing 50 nm Ti on the silicon substrate and then sputtering 200 nm Au on the titanium layer. The samples were heated up to 400 °C and then held at this temperature. Simultaneously, chronoamperometry was performed at a potential of −0.7 V. At this potential, titanium oxide is thermodynamically stable, leading to the oxidation of titanium atoms reaching the surface. In contrast, the gold layer remains metallic at the selected potential. As a consequence, the measured anodic current is a measure of the diffusion of the less noble metal through the more noble metal. Fig. 7a shows the current over time. The red line marks the time when the final temperature of 400 °C was reached. The reference electrode is not in equilibrium at lower temperatures and consequently the potential of the RE is not stable. Therefore, during heating, neither the potential nor the current is precisely defined [31]. After the temperature stabilizes at 400 °C, the reference electrode equilibrates. The heating process causes a negative current peak, but this is not related to the diffusion process. The same behavior is observed when measuring pure gold samples without a titanium layer. At 1275 s, a sharp increase in current can be observed. The current increase marks the point when the first titanium atoms reach the surface and are oxidized. The onset of the current increase is the time lag, tlag. The apparent diffusion coefficient D can be calculated using the formula $D = l^2/6t_{lag}$, where l is the thickness of the gold layer [32]. At around 1700 s, a plateau is reached, where the diffusion of titanium and its oxidation are in equilibrium. The gray shaded area in Fig. 7a marks the time period during which the characteristic “S-shape” occurs. This current profile is typical for electrochemical diffusion and permeation [33]. After that the current slightly decreases. The freshly formed titanium oxide at the surface suppresses further diffusion, preventing the oxidation and reducing the current. The parabolic current decrease also indicates oxidic layer growth. After the diffusion process, a HT-CV scan was performed to clarify whether titanium is indeed responsible for the rise in current. In Fig. 7b the Ox1 and Red1 peaks of titanium are visible, confirming the presence of titanium at the interface to the electrolyte.

Before the electrochemical experiment at elevated temperatures, an unaltered gold surface is visible under the Raman microscope (Fig. 8a). After the diffusion process during the heat treatment, the whole surface exhibits an almost uniform blue-green layer (Fig. 8b). In accordance with the HT-CV, Raman spectroscopy indicates the presence of titanium dioxide (anatase). A difference in peak position is observed between the main phonon mode in the Raman spectrum of titanium dioxide at 150 cm^{-1} and that of YSZ at 155 cm^{-1} (Fig. 8c). Furthermore, the Raman mode at around 620 cm^{-1} is shifted to higher wavenumbers at the titanium sample. This shift indicates the presence of another anatase band at 635 cm^{-1} [27] which is superimposed with the YSZ one.

With our coupled method, diffusion can be determined qualitatively based on the time lag and the current plateau. (*In situ)* Raman spectroscopy yields analytical proof of the electrochemical observations. Further planned work on this topic focuses on quantification of diffusion at different temperatures and conducting depth-resolving analytical methods afterwards.

5. Conclusion

In this work, we demonstrate a novel method that couples high-temperature electrochemistry with Raman spectroscopy to investigate metal oxidation processes and diffusion phenomena without detaching

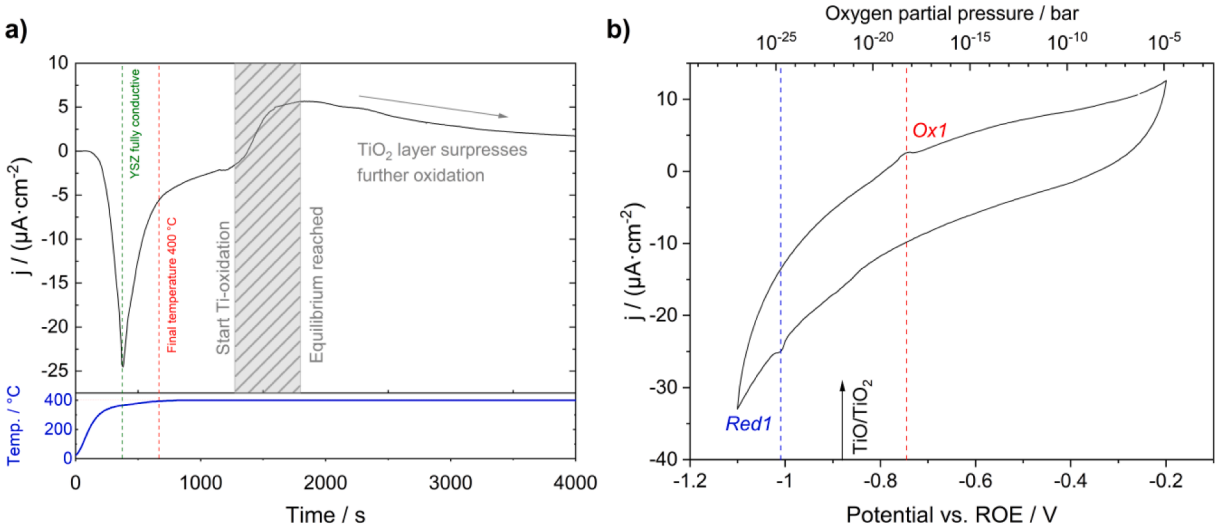

Fig. 7. a) Current and temperature over time. Different stages of the diffusion process are highlighted. b) CV after the diffusion process. The presence of titanium redox peaks confirms the presence of diffused titanium at the interface.

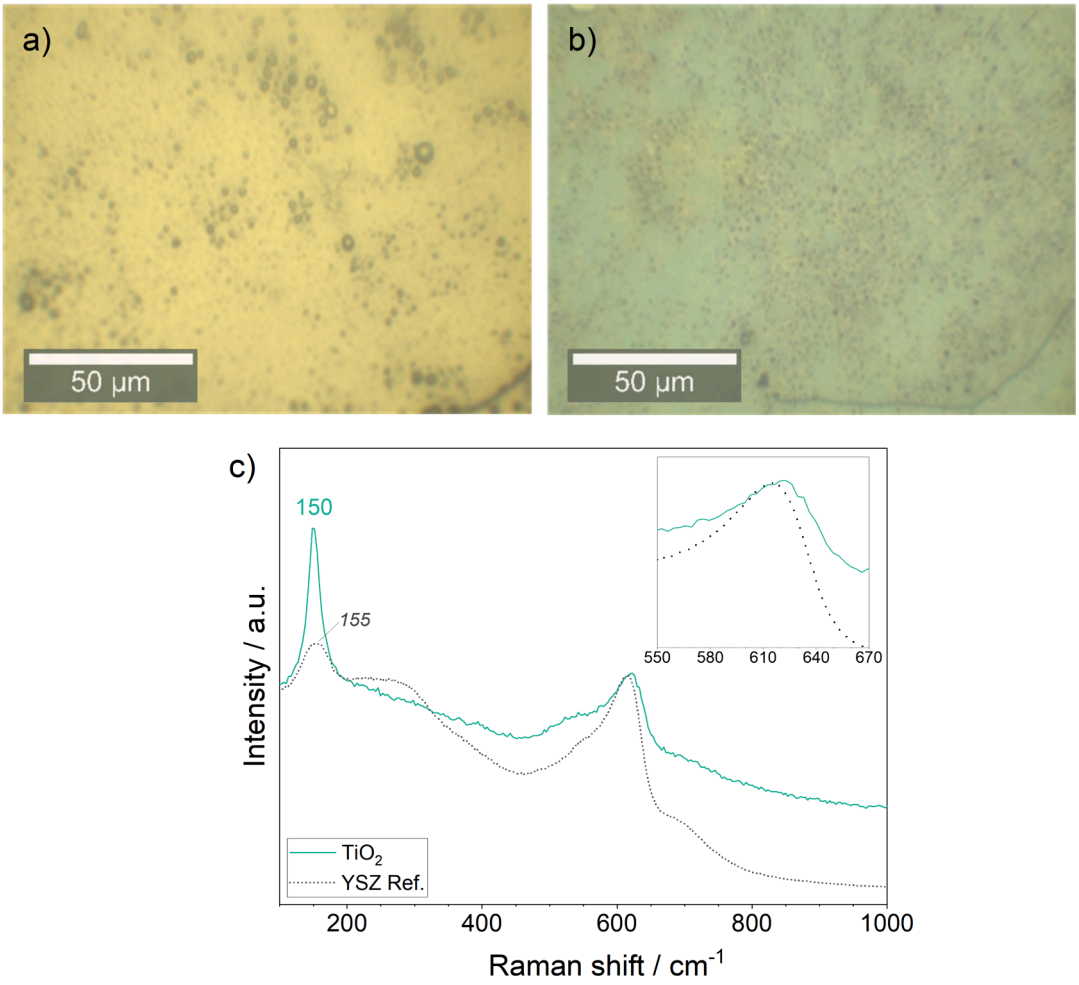

Fig. 8. a) Surface of the untreated sample. Only a pristine gold surface is visible. b) Surface after the heat-treatment/diffusion process. the surface is homogenously covered by a blue-green titanium dioxide layer. c) Raman spectrum of the surface after diffusion showing the major tio$_2$ Raman band and a slight shift of the Raman signal at around 620 cm^{-1}.

the metal electrode from the solid-electrolyte. High-temperature cyclic voltammetry is a suitable method for the controlled formation of defined oxides. For metals that have several oxidation stages, such as copper (Cu_2O and CuO), the different oxides can be formed in a targeted way. The reduction stability of the solid electrolyte (YSZ) poses a limit on measurable reduction processes. As a result, metals with a high affinity for oxygen, such as titanium, cannot be reduced back to their metal form once they have been oxidized. At the other end of the potential window, the oxidation process is limited by the oxygen evolution reaction. This means that the oxidation of noble metals like gold cannot be investigated with HT–CV.

In electrochemical experiments it is sometimes difficult to assign observed currents to specific reactions. Analytical validation of the formed products is essential. At high temperatures and subsequently weaker Raman Stokes scattering, the oxide bands are entirely overlaid by the YSZ. However, a method to work around this problem has been found. The defined oxidic states from HT-CV can be preserved by electrochemically maintaining the oxygen partial pressure during cooling. Raman spectroscopy of the thereby preserved defined oxides at room temperature reveals their chemical composition. *In operando* optical microscopy, during the electrochemical measurements, can also be used to visually confirm the different oxides through respective color changes on the surface.

The introduced method can also be applied to determine the diffusion of metals through other metal layers. It is limited to the diffusion of base metals through more noble metals, as the surface must remain in a metallic state at the set potential. The breakthrough time, extracted from the current–time plot can be used for the calculation of the diffusion coefficient. Raman spectroscopy can be used to verify the observed oxide species. Hence, the combination of HT-CV and Raman spectroscopy provides a versatile method for studying metal oxidation and diffusion processes of various metals through metal layers.

CRediT authorship contribution statement

Michael Georg Stadt: Writing – original draft, Investigation, Formal analysis. **Silvia Larisegger:** Writing – review & editing, Project administration. **Michael Nelhiebel:** Writing – review & editing, Funding acquisition. **Günter Fafilek:** Writing – review & editing, Formal analysis.

Declaration of competing interest

The authors declare that they have no known competing financial interests or personal relationships that could have appeared to influence the work reported in this paper.

Acknowledgements

This work was funded by the Austrian Research Promotion Agency (FFG, Project No. 905107). The authors acknowledge TU Wien Bibliothek for financial support through its Open Access Funding Program.

References

[1] B. Abd-El-Nabey, S. El-Housseiny, A. Abdel-Gaber, M. Mohamed, Kinetics of oxidation of metals in the air at room temperature using EDX, Results Chem. 5 (2023) 100876.

[2] Z. Grzesik, M. Migdalska, Oxidation Mechanism of Cu2O and Defect Structure of CuO at High Temperatures, High Temp. Mater. Processes 30 (4–5) (2011).

[3] S. Kavunga, G. Luckeneder, E.D. Schachinger, J. Faderl, G. Fafilek, In situ characterization of galvanized low-alloyed steels with high-temperature cyclic voltammetry during annealing, Electrochim. Acta 424 (2022) 140653.

[4] J. Öijerholm, G. Fafilek, J. Pan, Study of initial oxidation of engineering alloys by high-temperature cyclic voltammetry, Electrochem. Solid St. 10 (6) (2007) C47–C.

[5] P.A. van Manen, R. Weewer, J.H.W. de Wit, High temperature cyclic voltammetry on metal/metal oxide systems, J. Electrochem. Soc. 139 (4) (1992) 1130–1134.

[6] S. Kavunga, G. Fafilek, G. Luckeneder, E.D. Schachinger, K.-H. Stellnberger, J. Faderl, In situ study of selective manganese oxidation on low-alloyed steel using high-temperature cyclic voltammetry, Solid State Ion. 371 (2021) 115770.

[7] Y. Deng, A.D. Handoko, Y. Du, S. Xi, B.S. Yeo, In situ Raman spectroscopy of copper and copper oxide surfaces during electrochemical oxygen evolution reaction: identification of CuIII oxides as catalytically active species, ACS Catal. 6 (4) (2016) 2473–2481.

[8] S. Kanamori, H. Sudo, Effects of titanium layer as diffusion barrier in Ti/Pt/Au beam lead metallization on polysilicon, IEEE Transactions on Components, Hybrids, and Manufacturing Technology 5 (3) (1982) 318–321.

[9] W.E. Martinez, G. Gregori, T. Mates, Titanium diffusion in gold thin films, Thin Solid Films 518 (10) (2010) 2585–2591.

[10] I. Shalish, Y. Shapira, Thermal stability of a Ti-Si-N diffusion barrier in contact with a Ti adhesion layer for Au metallization, Journal of Vacuum Science & Technology B: Microelectronics and Nanometer Structures Processing, Measurement, and Phenomena 17 (1) (1999) 166–173.

[11] R. Wenzel, F. Goesmann, R. Schmid-Fetzer, Diffusion barriers in gold-metallized titanium-based contact structures on SiC, J. Mater. Sci. Mater. Electron. 9 (2) (1998) 109–113.

[12] G. Ashwell, R. Heckingbottom, Interdiffusion of titanium and gold: a comparison of thin films deposited in technical vacuum and ultrahigh vacuum, J. Electrochem. Soc. 128 (3) (1981) 649.

[13] W. Sylwestrowicz, H. Elkholy, G. Kammlott, The effect of temperature and humidity on interdiffusion of gold and titanium in thin films, J. Mater. Sci. 14 (1979) 873–881.

[14] X. Vendrell, A.R. West, Electrical properties of yttria-stabilized zirconia, YSZ single crystal: local AC and long range DC conduction, J. Electrochem. Soc. 165 (11) (2018) F966.

[15] G. Fafilek, Voltammetry on BICUVOX. 10 microsamples, Solid State Ion. 113 (1998) 623–629.

[16] S. Margueron, A. Bartasyte, Temperature-dependent resonant Raman scattering of yttria doped zirconia phases in thermal barrier coatings, J. Eur. Ceram. Soc. 44 (1) (2024) 419–425.

[17] D.R. Lide, Standard Thermodyanmic Properties of Chemical Substances, CRC Handbook of Chemistry and Physics, CRC Press (2004), 5–4–5-24.

[18] M.G. Stadt, M. Nelhiebel, S. Larisegger, G. Fafilek, In-situ Impedance Spectroscopy on Copper Oxide Scales under Potential Controlled Oxidation at High Temperatures, [Manuscript submitted for publication] (2023).

[19] T. Ha, I. Park, K.I. Sim, H. Lee, J.-S. Bae, S.J. Kim, J.P. Kim, T.-T. Kim, J.H. Kim, J. I. Jang, Single-crystalline Cu2O thin films of optical quality as obtained by the oxidation of single-crystal Cu thin films at low temperature, APL Mater. 7 (3) (2019).

[20] W. Wang, Q. Zhou, X. Fei, Y. He, P. Zhang, G. Zhang, L. Peng, W. Xie, Synthesis of CuO nano-and micro-structures and their Raman spectroscopic studies, CrstEngComm 12 (7) (2010) 2232–2237.

[21] N. Mironova-Ulmane, A. Kuzmin, I. Sildos, L. Puust, J. Grabis, Magnon and phonon excitations in nanosized NiO, Latv. J. Phys. Tech. Sci. 56 (2) (2019) 61–72.

[22] J. Krýsa, H. Krýsová, Z. Hubička, Š. Kment, J. Maixner, L. Kavan, Transparent rutile TiO 2 films prepared by thermal oxidation of sputtered Ti on FTO glass, Photochem. Photobiol. Sci. 18 (2019) 891–896.

[23] L. Kavan, N. Tétreault, T. Moehl, M. Grätzel, Electrochemical characterization of TiO2 blocking layers for dye-sensitized solar cells, J. Phys. Chem. C 118 (30) (2014) 16408–16418.

[24] R. Padma, K. Ramkumar, M. Satyam, Growth of titanium oxide overlayers by thermal oxidation of titanium, J. Mater. Sci. 23 (1988) 1591–1597.

[25] L. Kavan, Lithium insertion into TiO 2 (anatase): electrochemistry, Raman spectroscopy, and isotope labeling, J. Solid State Electrochem. 18 (2014) 2297–2306.

[26] R. Palomino-Merino, P. Trejo-Garcia, O. Portillo-Moreno, S. Jiménez-Sandoval, S. Tomás, O. Zelaya-Angel, R. Lozada-Morales, V. Castaño, Red shifts of the Eg (1) Raman mode of nanocrystalline TiO2: Er monoliths grown by sol–gel process, Opt. Mater. 46 (2015) 345–349.

[27] O. Frank, M. Zukalova, B. Laskova, J. Kürti, J. Koltai, L. Kavan, Raman spectra of titanium dioxide (anatase, rutile) with identified oxygen isotopes (16, 17, 18), PCCP 14 (42) (2012) 14567–14572.

[28] J. Choi, S.J. An, Backside metallization of Ag–Sn–Ag multilayer thin films and die attach for semiconductor applications, J. Electron. Mater. 49 (2020) 4265–4271.

[29] M. Fugger, M. Plappert, C. Schäffer, O. Humbel, H. Hutter, H. Danninger, M. Nowottnick, Comparison of WTi and WTi (N) as diffusion barriers for Al and Cu metallization on Si with respect to thermal stability and diffusion behavior of Ti, Microelectron. Reliab. 54 (11) (2014) 2487–2493.

[30] W.-F. Wu, K.-C. Tsai, C.-G. Chao, J.-C. Chen, K.-L. Ou, Novel multilayered Ti/TiN diffusion barrier for Al metallization, J. Electron. Mater. 34 (2005) 1150–1156.

[31] G. Fafilek, Automated device for electrochemical measurements and application to the system Pt/solid electrolyte, Solid State Ion. 86–88 (1996) 1415–1419.

[32] J. Crank, The mathematics of diffusion, Oxford University Press, 1979.

[33] M. Devanathan, Z. Stachurski, The adsorption and diffusion of electrolytic hydrogen in palladium, Proc. R. Soc. Lond. A 270 (1340) (1962) 90–102.